Pak. J. Chem. 14(1-2): 18-30, 2024 Research Article
ISSN (Print): 2220-2625
ISSN (Online): 2222-307X DOI: 10.15228/2024.v14.i1-2.p03

Experimental Study for the Influence of Methyl Substituent's Position on Quinoline for Inhibition of Aluminium Corrosion in Hydrochloric Acid

[1*]A.M. Usman, [2]J. Ambreen, [3]A.A. Muhammad, [4]N.U. Shehu and [5]M. U. Sadiq

[1]Department of Chemistry, Federal College of Education (Technical) Bichi, P.M.B. 3473, Kano, Nigeria
[2]Department of Chemistry, COMSATS University Islamabad, Park Road, 45550, Islamabad, Pakistan
[3,4]Department of Pure and Industrial Chemistry, Bayero University, PMB 3011, Kano. Nigeria.
[5]Quaid-i-Azam University Islamabad, 45320, Islamabad, Pakistan
Corresponding author. Email: amusman.se@fcetbichi.edu.ng,

Abstract

Some selected methylquinolines' performance on inhibition of Aluminum (Al) corrosion and the effect of methyl group at 5,7 and 8 on quinoline investigated in hydrochloric acid experimentally through weight loss, EIS (Impedance Measurement) and PDP (Potentiodynamic Polarization). For weight loss, five-methyl quinoline (5-MeQ), seven-methyl quinoline (7-MeQ) and eight-methyl quinoline (8-MeQ) were used in varying mass and temperature in different concentrations of HCl. The adsorption characteristics of these inhibitors were found to be consistent with Langmuir isotherm; both physical and chemical mechanisms played a significant role. Comparatively, the rate of corrosion, mass loss, inhibition effectiveness, and the degree of surface coverage obtained from the weight loss indicated the superiority of 5-MeQ performance over 7-MeQ and 8-MeQ. The eight-methyl quinoline has the least corrosion inhibition performance under the same conditions. The speed of the inhibition process was found to follow first-order kinetics for all the systems. The surface morphology and the functional group before and after the corrosion were investigated through SEM and FTIR analysis. The Nyquist plot from impedance data and the parameters also indicated the same behaviour as the weight loss. The Tafel plot polarization data and the parameters show the same trends. The results of the EIS. and PDP are found to be relatively consistent with that of weight loss. All the molecules showed outstanding corrosion inhibition efficiency. However, the 5-MeQ molecule gives better Al corrosion inhibition than the other two molecules.

Keywords: methylQuinoline, Al, corrosion, substituent, position

1. INTRODUCTION

The extraction of Al from its ore (bauxite) is virtually energy-extensive and economically expensive, necessitating the need for protection against severe corrosion problems. Nowadays, the use of acidic media in pickling, facility cleaning and descaling is indispensable in many industries [1]. Hydrochloric acid is a common acidic medium for these purposes because it is more economical, efficient and less troublesome compared to other mineral acids[2]. Even though Al is effectively inert in a neutral aqueous environment, it is strongly predisposed to corrosion in acidic media, even as dilutes as acid rainwater. In actual fact, Cl^- from various sources, including neutral salts, can cause pitting corrosion at vulnerable spots of passive film-protected non-ferrous metal [3]. A detailed literature search showed that Al and its oxides were investigated extensively against the corrosive action of chloride ions in an aqueous medium. A significant number of inhibitors have been studied, and several of their actions with regard to the corrosion inhibition of Al have been reported in the literature[4-7]. Organic corrosion inhibitors are preferred because they are environmentally friendly and effective at a wide range of temperatures[4]. The effectiveness of an organic inhibitor (molecule) depends on the size, aromaticity, type of functional groups, number of bonding atoms (π and σ bonds), nature and surface charge, the distribution of charge in the molecule and the type of aggressive media[4]. The presence of polar functional groups with S, O or N atoms in the molecule, heterocyclic compounds, and π electrons present in the molecule also upsurges the efficiency of these organic corrosion inhibitors[5,6]. The use of computational chemistry like Density Functional Theory (DFT), Molecular Dynamic simulation (MD), Monte Carlo (MC) simulation and Quantitative Rtructure-Activity Relationship (QSAR) modelling has been applied for the study of corrosion inhibition properties of organic molecules. Aromatic rings have mostly been regarded as the zones through which specific inhibitors can protect the etching of metals. The functional group attached to the aromatic ring also has a significant role in the corrosion inhibition of metals generally[7].

Methylquinolines are nitrogenous bicyclic heterocyclic compounds with a molecular formula of C_9H_9N; as such, it is expected to show reasonably good effectiveness against metallic corrosion because of their association with high electron density (10-π and 2-non bonding electrons)[8]. Quinoline derivatives containing polar substituents such as methyl ($-CH_3$) can effectively adsorb and form highly stable chelating complexes with surface metallic atoms through coordination bonding[8]. The available studies for corrosion inhibition of quinoline molecules focus on the nature and type of functional groups (being substituted or non-substituted) attached to the molecule in use. To our knowledge, this is the first investigation into the effect of the position of substituent groups in corrosion inhibition for Al in an acidic environment. However, aside from aromaticity, functional group and the type of substituent, corrosion inhibition efficiency of the heterocyclic compound can also be influenced by the nature and position of the substituent attached to the molecule [9]. This study is aimed at justifying the claim, which is very scanty or non-existent in the literature.

2. Materials And Methods

2.1. Materials

The inhibitors, which are the quinoline derivatives (5-methyl quinoline (5-MeQ), 7-methyl quinoline (7MeQ) and 8-methyl quinoline (8-MeQ)) (Fig. 1a-c) three in number, were obtained from the Aldrich Chemical Co. Ltd, (Gillingham Dorset - England), all with 99% purity. The inhibitors were used without further purification. Other materials are double distilled water-ethanol, with 96% purity; hydrochloric acid, with 37% purity and specific gravity of 1.175-1.185 g/20^{o}C; and acetone, with 99.5% purity and specific gravity of 0.713-0.714. The Al plate used in this study was composed of 98.9% Al, 0.5% Fe and 0.48% Si with traces of other elements, which include Ti, V, Mn, Ni Cu, Ga, etc, in negligible amounts, falling within the class of wrought Al. The metal coupons used in this experiment were mechanically cut and optimized (5.0cm × 3.0cm × 0.11cm) degreased in ethanol, rinsed in acetone, air-dried and preserved in moisture-free desiccators prior to corrosion study[10]. All test solutions for the corrodent purchased from Sigma-Aldrich were prepared by diluting 37% HCl in double distilled water.

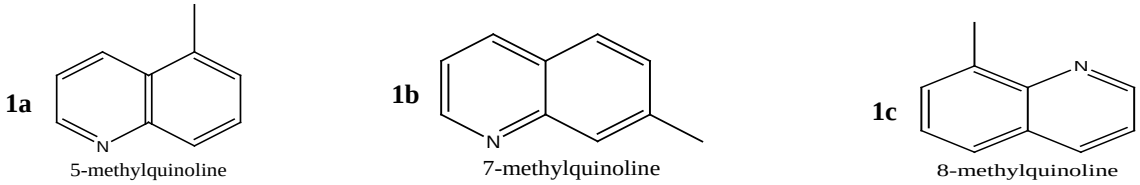

Figure 1a: methyl substituted quinoline at carbon 5; **1b**: methyl substituted quinoline at carbon 7; **1c**: methyl substituted quinoline at carbon 8

2.2. Mass Loss Measurement:

The metal coupons (5.0 cm × 3.0 cm × 0.11 cm) obtained were initially weighed suspended with the aid of Pyrex glass hooks tightened on a rod horizontally placed end to end held by retort stands such that 4.0 cm × 3.0 cm of the test metal is immersed each in 80ml of 0.2M, 0.4M and 0.6M HCl solution containing different concentrations of inhibitor (0.0, 0.2, 0.4, and 0.6 g/L). Contact was allowed for 5 h at 303, 313 and 323K. The coupons were then withdrawn at predetermined intervals of time, washed, rinsed in acetone, dried, and reweighed, and then mass losses were recorded. The above procedure was tested for all three quinoline derivatives in triplicates. The mass measurements were performed on the Mettler FA2004 electronic balance. From the mass loss data, corrosion rate (CR, in $gh^{-1}cm^{-2}$), the degree of surface coverage (θ) and Inhibition efficiency I (%) were computed using the following equations (1-4) :

$$\text{Weight Loss} = W_1 - W_2 \quad (1)$$

$$\theta = 1 - \frac{W_1}{W_2} \quad (2)$$

$$\%\ IE = \left(1 - \frac{W_1}{W_2}\right) \times 100 \quad (3)$$

$$CR\ (gh^{-1}cm^{-2}) = \frac{\Delta W}{At} \quad (4)$$

Where W_1 is the initial masses (g) of Al and W_2 is the final mass after time t, θ is the degree of surface coverage of the inhibitor, A is the area of the Al coupon (cm^2), t is the immersion time (h)[11].

2.3. Electrochemical Measurements:

2.3.1. Impedance Measurement (EIS):

Electrochemical Impedance tests were carried out at 303 ± 1K in a three-electrode cell using a Gamry interface 5000E potentiostat (Louis Drive Warminster, PA 18974, USA) equipped with complete Gamry framework version 7.9.0 and Gamry Ecchm Analyst version7.9.0, with V_3 Studio software over a frequency range of 100 kHz - 10 mHz, with a signal amplitude of 5mV. A graphite rod was used as a counter electrode, and a Ag/AgCl electrode was used as the reference electrode. The latter was connected via a Luggin's capillary. In a typical experiment, 0.4g/L 5-MeQ inhibitor was dispersed in 0.4M HCl by stirring with the aid of a magnetic stirrer prior to impedance measurements. The same procedure was followed using 7-MeQ and 8-MeQ inhibitors. Measurements were performed in aerated and unstirred solutions after 30 minutes of immersion in the test solutions. The working electrodes were prepared from square sheets of Al with 1cm^2 of the area exposed to the test solution [12]. Origin lab software was used for data handling, which gives the Nyquist plot for each system. The charge transfer resistance values were obtained from the diameter of the semicircles of the Nyquist plots. The inhibition efficiencies of the inhibitors were also calculated from the charge transfer resistance values [12].

2.3.2. Potentiodynamic Polarization (PDP):

Potentiodynamic polarization studies were performed in 0.4 M HCl at 303 K using a Gamry interface 5000E potentiostat (Louis Drive Warminster, PA 18974, USA) equipped with complete Gamry framework 7.9.0, having an acquisition system installed with NOVA software package version 1.8 and a three-electrode electrochemical cell: the metal coupons of surface area 1 cm^2 as working electrode, an Ag/AgCl reference electrode and a graphite counter electrode. Al samples for electrochemical experiments were of dimension 1.0 cm × 1.0 cm ×0.11 cm. These were subsequently sealed with epoxy resin in such a way that only one square surface of area 1.0 cm^2 was left uncovered. The exposed surface was degreased in

acetone, rinsed with distilled water, and air-dried. The Al metal was polarized between –1,000 and 2,000 mV at a specific scan rate of 0.333 mVs^{-1} and 303K. From the polarization test data for inhibited Al in an acid medium, the electrochemical parameters such as Tafel slopes, corrosion potential, corrosion current and corrosion rate were calculated. The linear region of anodic and cathodic curves was extrapolated with a 0.0016V/sec scan rate. From the Tafel analysis, corrosion current density, corrosion rate, linear polarization resistance and corrosion potential were obtained in a static solution [13]. The inhibition efficiency IE (%) was also computed, and each test was run in triplicate. Measurements were performed in 0.4 M acid solutions containing 0.4 g/L mass of the test inhibitors [14]. The inhibition efficiency (% IE) was deduced from the linear polarization resistance (LPR) and potentiodynamic polarization-corrosion rate (PP-CR), which was used as criteria for the assessment of corrosion resistance of Al in corrosive environments using the following equation (Eqn.5):

$$\%IE = \frac{CR_o - CR}{CR_o} \times 100 \qquad (5)$$

Where CR_o and CR are the corrosion rates of the materials in the presence and absence of inhibitors [13].

2.4. Surface characterization:

To understand the type and nature of corrosion on the Al, the resulting surfaces, before and after corrosion, were examined on the Phenom ProX model (Netherlands) scanning electron microscope at accelerating voltages of 5.00kV. Infrared spectra of the adsorbed inhibitors were recorded using Shimadzu FTIR-8400S Fourier Transform Infrared Spectrometer (FTIR) over a frequency range of 400-4000cm^{-1}. Elemental analysis of Al test plates was performed on Mini Pal 4 PW 4030 energy dispersive X-ray fluorescence spectrometer (EDXRF) installed with Mini Pal analytical software. The specimens were stimulated by a potential of 30 kV and a current of 1 mA for 10 min.

3. Results and Discussion:

3.1. Weight Loss Analysis:

The corrosion inhibition performance profile of 5-MeQ, 7-MeQ and 8-MeQ systems for the anti-corrosion effect on Al via weight loss experiment is shown in Fig. (2 to 6). A progressive reduction in weight loss (Fig. 2) was observed with an increase in inhibitors masses (g/L) at 303K for all three systems (5-MeQ/0.2M HCl on Al, 7-MeQ/0.2M HCl on Al and 8-MeQ/0.2M HCl on Al) concurrently under the same condition. The vertical height of the bars in Fig. (2-4) is a function of the amount of weight lost by the Al in a test for the blank and the inhibited case for the system. This is in agreement with the fact that the presence of inhibitor molecules prevents the corrodent molecules (acid) from having complete contact with the metal surface such that a barrier has been created in between, which could be physically or chemically depending on the adsorption characteristics [15]. Here, it is assumed that without the inhibitor, the metal surface was like a smooth and flat surface. When the corrodent molecules collide with the metal surface, they have to overcome a lot of resistance to get past the surface and start the corrosion reaction. However, when an inhibitor is introduced, it behaves like a small bump on the surface of the metal[15]. The corrodent molecules can now get a better grip on the metal surface because of the inhibitor molecules. In this situation, the corrodent molecules don't have to overcome as much resistance to start the corrosion reaction.

Consequently, the presence of the inhibitor molecules effectively reduces the activation energy required for the reaction to occur. The variation of the inhibitor mass from 0.0 through 0.2, 0.4 to 0.6g/L shown in Fig. (2-4) profile leads to a decrease in mass loss of the Al at all temperatures and all corrodent concentrations. This is because the increase in the inhibitor mass leads to a rise in the number of inhibitor molecules available to interact with the corrodent molecules and reduce the activation energy[16]. It's just like putting more bumpers on the metal surface to make it easier for the corrodent molecules to attach. Also, Fig. (2-4) gave a clear situation for the effect of varying temperature from 303K, 313K and 323K. There's an increase in weight loss of the metal as the temperature increases. This has been reported by many scholars [16]. It's because, at elevated temperatures, the inhibitor molecules become segregated and more porous on the metal surface[17]. This allows some contact between the metal and the corrodent molecules, hence causing more mass loss than at room temperature.

Another observable effect from Fig. (2-4) is that 5-MeQ has the lowest weight loss (shortest bar) for all the inhibitor mass at all temperatures. This is a clear indication that 5-MeQ is more adsorbed on the metal surface than the remaining inhibitors, and so regardless of the inhibitor dose applied, 5-MeQ exhibits relatively lower mass loss compared to 7-MeQ and 8-MeQ, indicating clearly its superior anti-corrosion efficiency.

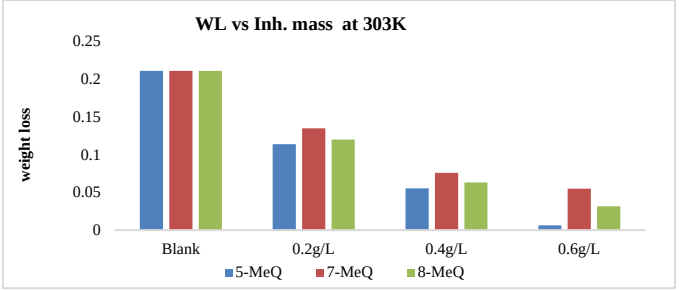

Figure 2: Weight loss of Al in 0.2M HCl at 303k using 5-MeQ, 7-MeQ and 8-MeQ inhibitors with varying mass for each system.

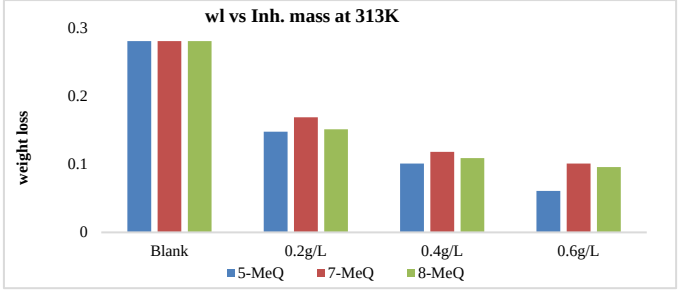

Figure 3: Weight loss of Al in 0.2M HCl at 313k using 5-MeQ, 7-MeQ and 8-MeQ inhibitors with varying mass for each system.

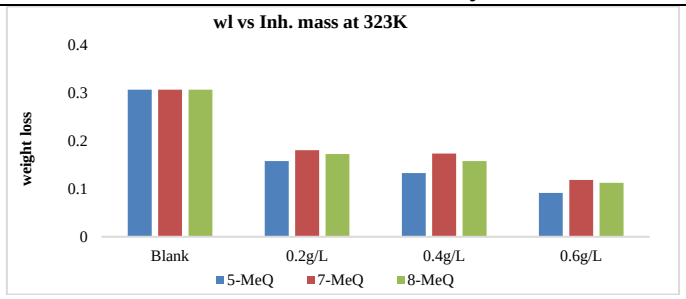

Figure 4: Weight loss of Al in 0.2M HCl at 323k using 5-MeQ, 7-MeQ and 8-MeQ inhibitors with varying mass for each system.

Figures (5 & 6) show an increase in corrodent concentration with an increase in mass loss of the metal serially, irrespective of temperature and inhibitor mass. Corrosion was more rapid in 0.6M, followed by 0.4M and 0.2M, with the lower corrosion of metal both in the absence and in the presence of inhibitor at all temperatures. It may be attributed to the breakdown of the air-formed passive film and the initiation of pitting, which is traditionally followed by steady-state corrosion conditions due to cathodic reaction [18]. In most cases, the reason for varying the concentration of the corrodent in corrosion inhibition study is to allow the study of how the adsorption behaviour changes with the corrosiveness of the environment[18]. It will also help determine the optimal concentration of inhibitors for a given level of corrosion. As the concentration of the corrodent increases, the activation energy for the reaction decreases. It was because there were more corrodent molecules available to react, so they could provide more energy to overcome the energy barrier and start the reaction[18].

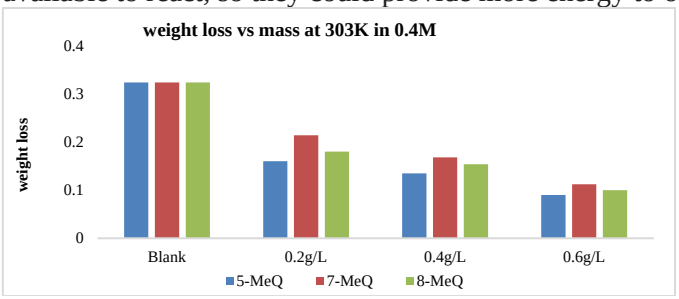

Figure 5: Weight loss of Al in 0.4M HCl at 303k using inhibitors 5-MeQ, 7-MeQ and 8-MeQ with varying mass for each system.

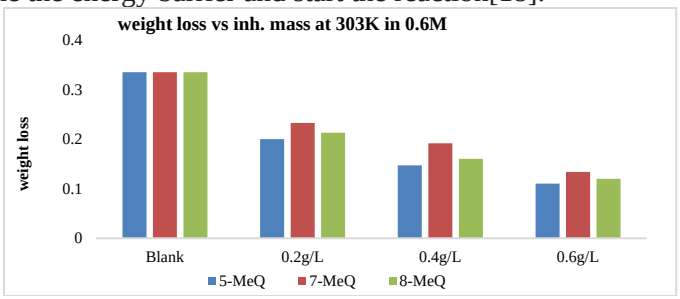

Figure 6: Weight loss of Al in 0.6M HCl at 303k using inhibitors 5-MeQ, 7-MeQ and 8-MeQ with varying mass for each system.

3.2. Corrosion rate analysis:

Corrosion rate is a measure of how quickly a material corrodes or goes into solution[19]. It can be expressed in terms of the amount of material lost over time, such as milligrams per square meter per day. Corrosion rate is an essential factor to consider when studying corrosion inhibition, as the goal generally is to reduce the rate of corrosion[19]. Figure (7) is the profile of the corrosion rate in 0.2MHCl at 303K with varying inhibitor mass for each system. It can be observed from Fig.(7) that the rate of attack slows down in the presence of inhibitors. As the concentration of the corrosion inhibitor increases, the corrosion rate tends to decrease[20]. This is because the inhibitor molecules adsorbed onto the metal surface form a protective layer that prevents the metal from coming in contact with the corrosive environment [20]. The protective layer becomes thicker as the number of inhibitor molecules increases; consequently, the corrosion rate will reduce. Fig. (7) indicates that the corrosion rate is slower, with 5-MeQ as the inhibitor, which is the inhibitor with a shorter bar. 5-MeQ has been observed to be more attracted to the metal surface than other inhibitors used here. In this study, the corrosion rate is in the order 8-MeQ > 7-MeQ > 5-MeQ. The molecules have the same molecular mass and an equal number of atoms, but there's a noticeable difference in terms of performance in the reduction of corrosion rate among them. This suggests that the position of the methyl substituent on the parent quinoline may be responsible for the difference in corrosion inhibition efficiency due to the difference in molecular stability.

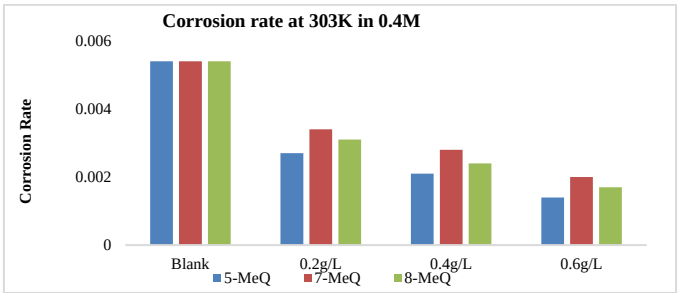

Figure 7: Corrosion Rate of Al in 0.2M HCl at 303k with varying inhibitor mass for each system.

The percentage inhibition efficiencies (% IE) in 0.2M HCl at 303K, 313K and 323K, respectively, with varying inhibitor mass for each system, are shown in Fig. (8-10). The inhibition efficiency of the molecule (inhibitor) is the percentage reduction in the corrosion rate when a corrosion inhibitor is added [21]. Fig. (8-10) shows an increase in the vertical height of the bar with an increase in the inhibitor mass for each of the inhibitors, which is the direct increase in the percentage inhibition efficiency as the mass of the inhibitor is increased at all temperatures. Also, here, unlike the weight loss and the corrosion rate, the percentage inhibition efficiency increased with an increase in the inhibitor mass and decreased with elevation of temperature[21]. Also, despite the fact that the three molecules used, 5-MeQ, 7-MeQ, and 8-MeQ, are comparably of the same molecular mass and number of atoms, observably, the molecule 5-MeQ has the highest percentage inhibition efficiency followed by 8-MeQ with 7-MeQ having the least. This can also be observed in Table (1), which indicates the variation of inhibitor mass and temperature in 0.2M HCl. Both the values of the mass loss and the percentage inhibition efficiency are consistent with Fig (2-7). There are possible reasons for the difference in the corrosion rate and the percentage inhibition efficiencies among the three molecules, which will be discussed after further consideration of other experimental results (PDP and EIS) and the quantum chemical parameters here.

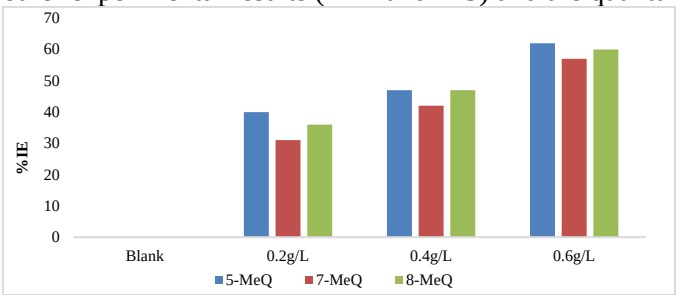

Figure 8: %IE for corrosion of Al in 0.2M HCl at 303k with varying inhibitor mass for each system.

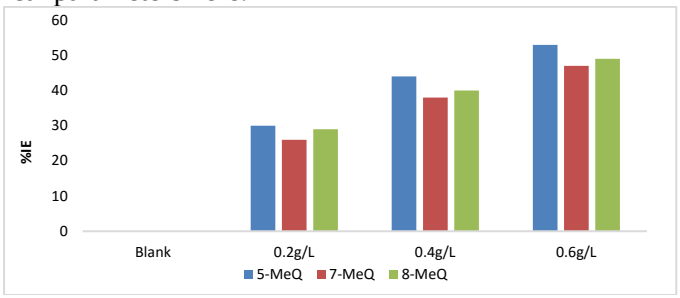

Figure 9: %IE for corrosion of Al in 0.2M HCl at 313k with varying inhibitor mass for each system.

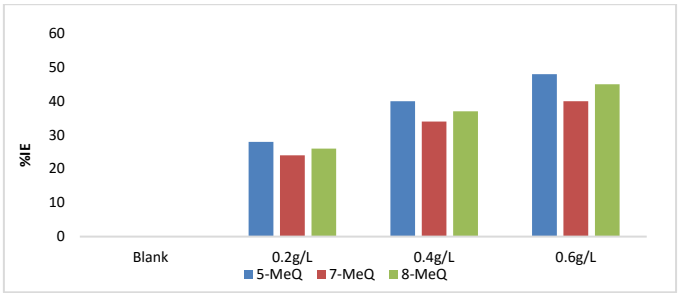

Figure 10: %IE for corrosion of Al in 0.2M HCl at 323k with varying inhibitor mass for each system.

Table 1: Mass loss of the Al and the inhibition efficiency of each inhibitor with varying masses in 0.2M Hydrochloric Acid (Corrodent) at 303K, 313K and 323K.

S/N	Inhibitor	Conc.g/L	Average mass loss (g) at 303K	%IE	Average mass loss (g) at 313K	%IE	Average mass loss (g) at 323K	%IE
	Blank	0	0.2110	0	0.2810	0	0.3061	0
1	5-MeQ	0.2	0.1101	52	0.1343	48	0.1401	38
		0.4	0.0511	76	0.1002	59	0.1211	55
		0.6	0.0114	98	0.0501	73	0.0931	67
2	7-MeQ	0.2	0.125	33	0.1759	30	0.1854	28
		0.4	0.0740	55	0.1188	41	0.1635	37
		0.6	0.0419	66	0.0778	50	0.1124	49
3	8-MeQ	0.2	0.1206	47	0.15	33	0.1602	31
		0.4	0.0615	61	0.1102	46	0.1312	46
		0.6	0.0201	85	0.0701	56	0.1102	54

Table (1) clearly shows the increase in mass loss with an increase in temperature and the decrease in mass loss with an increase in inhibitor concentration, which has also been reported by many authors [22]. From the observation of the parameters in Table (1), 5-MeQ has the better inhibitive performance, followed by 8-MeQ, and 7-MeQ has the lowest performance under the same conditions. In general, the act of corrosion inhibitor molecules for Al in an HCl environment is exceptional. The prime goal of using corrosion inhibitors is to stop or minimize the extent of severe chemical attacks on the metal surface to a reasonable percentage, thus mitigating economic and social consequences[22].

3.3. Kinetic study:

Results reported in Table (2) display complete information about kinetic parameters obtained from weight loss experiments that investigated Al corrosion in HCl solutions utilizing hydroxyquinolines at various temperatures. The value of the rate constant and R^2 are the parameters for establishing the kinetics of chemical reactions at varying temperatures [23]. In almost all systems, the R^2 values are closer to unity for the first-order results than that of the second-order and have higher values of the rate constant.

Table 2 : Kinetics for Corrosion of Al using 0.4g s of each inhibitor in 0.4M Hydrochloric Acid (Corrodent) at varying temperatures.

	Inhibitor		**5-MeQ**			
Temp.	303K		313K		323K	
	k_1	R^2	k_1	R^2	k_1	R^2
1st order	0.018	0.999	0.022	0.998	0.025	0.997
2nd order	0.001	0.542	0.004	0.239	0.005	0.498
	Inhibitor		**7-MeQ**			
Temp.	303K		313K		323K	
	k_1	R^2	k_1	R^2	k_1	R^2
1st order	0.016	0.999	0.020	0.999	0.024	0.998
2nd order	0.001	0.352	0.003	0.697	0.005	0.696
	Inhibitor		**8-MeQ**			
Temp.	303K		313K		323K	
8-OHQ	k_1	R^2	k_1	R^2	k_1	R^2
1st order	0.016	0.997	0.021	0.998	0.022	0.999
2nd order	0.001	0.342	0.003	0.568	0.004	0.698

This confirmed the fact that the corrosion inhibition of Al with hydroxyquinolines followed the first-order kinetic. The first and the second-order kinetic rate constant was obtained using equations (6 and 7)

$$-\frac{1}{t}\text{In}\frac{[A]}{[Ao]} = k_1(s^{-1}) \quad \text{or} \quad \frac{1}{t}\text{In}\frac{[Ao]}{[A]} = k_1 \qquad (6)$$

$$\frac{1}{[A]} = k_2 t + \frac{1}{[Ao]} \qquad (7)$$

Where $[A_o]$ is the initial mass of the metal, [A] is the mass corresponding to time t, k_1 and k_2 are the first and second-order rate constant, respectively [23].

3.4. Activation parameters:

The values of activation energies and heat of adsorption were determined under varied temperatures on Al corrosion within diverse HCl concentrations, each containing dissimilar inhibitor masses (Table 3). The following Arrhenius Equations were applied for this analysis.

$$CR = Aexp\left(\frac{-Ea}{RT}\right) \qquad (8) \qquad [24]$$

Taking the logarithm of both sides at a particular temperature gives Equation 9, while at two different temperatures gives equation (10) as follows:

$$\log(CR) = \log A - \frac{Ea}{2.303RT} \qquad (9) \qquad [24]$$

$$\log\left(\frac{CR_2}{CR_1}\right) = \frac{Ea}{2.303R}\left(\frac{1}{T_1} - \frac{1}{T_2}\right) \qquad (10) \qquad [10]$$

$$Q_{ads} = 2.303R\left[log\left(\frac{\theta_2}{1-\theta_2}\right) - log\left(\frac{\theta_1}{1-\theta_1}\right)\right] x \frac{T_1 x T_2}{T_2 - T_1} kJ/mol \qquad (11)$$

Where θ_1 and θ_2 are the degrees of surface coverage at the temperatures T_1 and T_2, respectively [26], at constant pressure, the value of Q_{ads} (11)approximates the enthalpy of adsorption (ΔH_{ads}).

The free energy change of adsorption, ΔG^o_{ads}, is calculated using equation (12) [26]:

$$\Delta G^0_{ads} = -RT \ln(55.5 \times K_{ads}) \qquad (12)$$

Where 55.5 is the molar concentration of water in the solution, R and T remain the same as described above, and K_{ads} was obtained from the intercept of a plot of θ against log$C$. For adsorption to take place, ΔG_{ads} must be negative. Now, ΔS_{ads} is always negative because the adsorbed atoms or molecules lose degrees of freedom in the process. As a result, ΔH_{ads} also supposed to be negative, showing that most of the adsorption processes are exothermic. Generally, the values of ΔG^0_{ads} around -20 kJmol^{-1} correspond to physisorption, while those above -40 kJmol^{-1} correspond to chemisorption [26]. The heat of adsorption Q_{ads}, which can also be defined by equation (10), depends on the energies of the bonds formed between the adsorbed atoms and the metal surface [27].

The activation energy is the minimum energy required for the corrosion reaction to occur, while the heat of adsorption is the energy released when the inhibitor molecules are adsorbed onto the metal surface. The activation energy is related to the overall corrosion reaction, while the heat of adsorption is specific to the interaction between the inhibitor molecules and

the metal surface[27]. Table (3) shows a decrease in activation energy with an increase in corrodent concentration without inhibitor. This is consistent with the theory of chemical reaction since the collision of molecules leads to chemical reactions.

Table 3: Activation Energy, E_a (kJ/mol) and Q_{ads} (kJ/mol) of Different Inhibitor Systems of 0.2, 0.4 and 0.6g/L on Al at 313K and 323K Obtained through Weight Loss Method.

	5-MeQ(g/L)							
	0.00		0.2		0.4		0.6	
Corrodent concentration	Ea	Qads	Ea	Qads	Ea	Qads	Ea	Qads
0.2M	33.05	0.00	12.98	-84.03	5.54	-93.99	4.17	-107.31
0.4M	28.18	0.00	17.29	-66.73	7.72	-78.35	5.31	-90.17
0.6M	23.25	0.00	19.61	-54.89	10.83	-63.63	7.78	-83.29
	7-MeQ(g/L)							
	0.00		0.2		0.4		0.6	
Corrodent concentration	Ea	Qads	Ea	Qads	Ea	Qads	Ea	Qads
0.2M	33.05	0.00	20.46	-27.86	18.31	-33.91	14.98	-65.69
0.4M	28.18	0.00	21.19	-23.66	17.21	-27.86	16.08	-57.22
0.6M	23.25	0.00	23.02	-19.64	21.16	-23.36	19.64	-33.68
	8-MeQ(g/L)							
	0.00		0.2		0.4		0.6	
Corrodent concentration	Ea	Qads	Ea	Qads	Ea	Qads	Ea	Qads
0.2M	33.05	0.00	19.66	-34.28	13.54	-41.01	11.03	-87.01
0.4M	28.18	0.00	20.54	-28.69	16.08	-33.66	14.97	-80.17
0.6M	23.25	0.00	22.66	-27.27	19.24	-29.81	18.46	-67.09

The gravity of this collision depends on the distance between the molecules [27]. When the concentration of the corrodent is increased, more molecules are introduced into the system, and the distance between them is shortened; hence, less energy is required for the activation of the reaction. Subsequently, the higher the concentration of the corrodent, the lower the activation energy for the corrosion reaction will be [29].

The difference in activation energy and heat of adsorption with and without an inhibitor suggests that the inhibitor is responsible for changing the mechanism of the corrosion [30]. Without an inhibitor, the rate of corrosion is directly proportional to the concentration of the corrodent, and there is no heat of adsorption because the corrodent is not forming a bond with the metal surface. As shown in Table (3), with an inhibitor, activation energy decreases as inhibitor mass increases, indicating that the inhibitor is lowering the barrier to the reaction and increasing the rate of corrosion. This could be due to the formation of a new bond between the inhibitor and the metal surface, which has a lower activation energy[29]. The increase in activation energy with increasing corrodent concentration when an inhibitor is present suggests that the inhibitor is creating a barrier that makes it harder for the corrodent to react with the metal surface. This could be due to the formation of the layer of inhibitor molecules on the metal surface that blocks the corrodent from reaching the surface[30].

The increase in the heat of adsorption also suggests that a bond is being formed between the inhibitor and the metal surface. Table (3) indicates that 5-MeQ has lower activation energy and higher heat of adsorption compared to the other molecules, followed by 8-MeQ and 7-MeQ, has the highest activation energy. This could be due to the unique structure of 5-MeQ, which allows it to interact with the metal surface in a way that lowers the energy barrier for the reaction. Results reported in Table (4) showed that as the corrodent concentration increases, the enthalpy of the system rises, which means that the system becomes more energetically and favourable for the corrosion reaction to take place.

Table 4: Enthalpy, ΔH_{ads} (kJ/mol) and Entropy, ΔS_{ads} (kJ/mol/K) Values Obtained with and without Different Inhibitors Systems of 0.2, 0.4 and 0.6g/L on Al through Weight Loss Method.

	5-MeQ(g/L)							
Corrodent concentration	0.00		0.20		0.40		0.60	
	ΔH_{ads}	ΔS_{ads}	ΔH_{ads}	ΔS_{ads}	ΔH_{ads}	ΔS_{ads}	ΔH_{ads}	ΔS_{ads}
0.2M	32.92	0.197	20.54	0.209	17.55	0.224	15.38	0.229
0.4M	42.28	0.182	25.92	0.201	21.63	0.201	18.32	0.217
0.6M	51.77	0.167	30.52	0.192	31.77	0.196	23.93	0.212
	7-MeQ(g/L)							
Corrodent concentration	0.00		0.20		0.40		0.60	
	ΔH_{ads}	ΔS_{ads}	ΔH_{ads}	ΔS_{ads}	ΔH_{ads}	ΔS_{ads}	ΔH_{ads}	ΔS_{ads}
0.2M	32.92	0.197	25.95	0.213	23.55	0.228	19.89	0.231
0.4M	42.28	0.182	32.39	0.209	28.63	0.213	23.28	0.220
0.6M	51.77	0.167	43.52	0.189	39.47	0.198	30.87	0.211
	8-MeQ(g/L)							
Corrodent concentration	0.00		0.20		0.40		0.60	
	ΔH_{ads}	ΔS_{ads}	ΔH_{ads}	ΔS_{ads}	ΔH_{ads}	ΔS_{ads}	ΔH_{ads}	ΔS_{ads}
0.2M	32.92	0.197	25.04	0.212	22.55	0.227	17.88	0.235

0.4M	42.28	0.182	30.39	0.204	27.37	0.211	23.28	0.224
0.6M	51.77	0.167	40.55	0.187	38.48	0.199	29.87	0.207

This is because the corrodent is the reactant in the corrosion reaction[31]. The decrease in ΔS_{ad} with increasing corrodent concentration is also an interesting issue since the system is becoming more ordered as the corrodent molecules are added. However, the opposite trends are observed for the system with inhibitor mass. This suggests that the inhibitor disturbs the corrosion reaction and makes the system less energitic[31]. The ΔH_{ads} and ΔS_{ad} values have opposite trends as the corrodent concentration increases. This is likely due to the fact that the inhibitor has two different effects on the system: i) it blocks the corrosion reaction, which decreases the system's enthalpy, and ii) it increases the disorder of the system, which increases the system's entropy which can be observed in Table (4). This is a fascinating example of how two opposing forces can have a complex interaction to determine the overall properties of the system. The ΔH_{ads} and ΔS_{ad} values for 5-MeQ have better precision than the other two inhibitors. This justifies the superiority of the 5-MeQ in terms of corrosion inhibition performance.

Generally, the inhibitor's effects on the corrosion reaction can be summarized in two main points. First, the inhibitor is blocking the reaction and preventing the loss of metal from the surface. Second, the inhibitor increases the disorder of the system, which may help to prevent the formation of corrosion products[32]. The overall effect of an inhibitor is to reduce the rate of corrosion reaction and to prevent the damage caused by corrosion. This is very useful in practical applications where corrosion prevention is essential [33]. The outcomes reported in Table (4) reveal that the difference seen in the inhibition efficiencies in Table (1) does not emerge from the size of the substituent but probably comes from the substituent position. In other words, the size of a substituent attached to quinoline has no significant effect on the corrosion inhibition of Al in an HCl solution. This reflects the characteristics of liquid or solid reactions likely to be Al dissolution due to ineffective inhibition [34].

3.5. Adsorption Study:

The adsorption isotherms provide valuable information on the nature of the interaction between the inhibitor molecules and the metal surface. The surface coverage (θ) of the adsorbed molecules can be determined by dividing the inhibition efficiency values of the weight loss runs by 100 [35]. The results obtained for θ were analyzed using Langmuir, Temkin, Flory Huggins and El-Awardy adsorption isotherm equations as given by equations (13- 16), respectively.

$$\frac{C}{\theta} = \frac{1}{K} + C \qquad (13)$$

$$\theta = \frac{-\ln\log K_{ads}}{2\alpha} - \frac{\ln C}{2\alpha} \qquad (14)$$

$$log\frac{\theta}{C} = \log K + x\ log\ (1-\theta) \qquad (15)$$

$$log\frac{\theta}{(1-C)} = logK + y\log C \qquad (16)$$

where C is the concentration of the inhibitor in g/L, and K_{ads} is the equilibrium constant of the adsorption process[35]. The Langmuir adsorption isotherm parameters are shown in Table (5). The linear regression coefficient is close to unity for almost all the inhibitors. The degrees of surface coverage, θ, at various concentrations of the selected quinolines at 303 and 323 K were the data used for plotting the isotherms. The data were tested using different adsorption isotherm equations (13-16), viz. Langmuir, Temkin, Flory-Huggins, and El-Awady show the parameters of linearisation of each adsorption model[36].

Table 5: Langmuir Adsorption Isotherm Parameters Obtained from the Adsorption of the Inhibitors on Al Surfaces at Different Temperatures.

Inhibitor		303K			313K			323K		
	Corr.Conc.	R^2	Slope	K_{ads}	R^2	Slope	K_{ads}	R^2	Slope	K_{ads}
5-MeQ	0.2MHCl	0.998	0.329	0.941	0.999	0.655	0.644	0.992	0.631	0.625
	0.4MHCl	0.846	0.490	0.692	0.995	0.529	0.646	0.878	0.463	0.639
	0.6MHCl	0.972	0.315	0.833	0.996	0.510	0.599	0.997	0.636	0.428
		303K			313K			323K		
	Corr.Conc.	R^2	Slope	K_{ads}	R^2	Slope	K_{ads}	R^2	Slope	K_{ads}
7-MeQ	0.2M HCl	0.997	0.414	0.869	0.999	0.592	0.620	0.997	0.666	0.517
	0.4M HCl	0.913	0.561	0.584	0.921	0.626	0.506	0.958	0.628	0.459
	0.6M HCl	0.990	0.313	0.791	0.989	0.527	0.515	1.000	0.517	0.435
		303K			313K			323K		
	Corr.Conc.	R^2	Slope	K_{ads}	R^2	Slope	K_{ads}	R^2	Slope	K_{ads}
8-MeQ	0.2MHCl	0.999	0.323	1.371	0.977	0.571	0.825	0.958	0.628	0.688
	0.4MHCl	0.993	0.403	0.830	0.997	0.412	0.777	0.964	0.459	0.683
	0.6MHCl	0.990	0.455	0.713	0.894	0.479	0.697	0.974	0.498	0.550

The surface coverage obtained from IE% values fitted all the adsorption models since the values of the regression coefficient, R^2, were mainly more excellent and close to unity in Langmuir for all three systems [38]. However, the Langmuir adsorption isotherm fitted the best, with almost all the systems having R^2 values close to unity. Sometimes, it may be sufficient to confirm inhibitor adsorption from data that fits the isotherms. Frequently, it is also desirable to extend the scope to include the deduction of thermodynamic parameters associated with the adsorption process using the relationship between the adsorption equilibrium constant (kads) and the standard free energy of adsorption, ΔGads[37].
Fig. (11) depicts the characteristics of impedance responses at the metal/acid interface for the corrosion of Al in the absence and in the presence of 0.4 g/L of each inhibitor in 0.4M HCl. The impedance spectra for the Nyquist plots of Al in the acid solutions in the absence and presence of the hydroxyquinolines were appropriately analyzed by fitting to the equivalent circuit model Rs (C_{dl} Rct), which has been previously used to model the metal/acid interface[37,38].

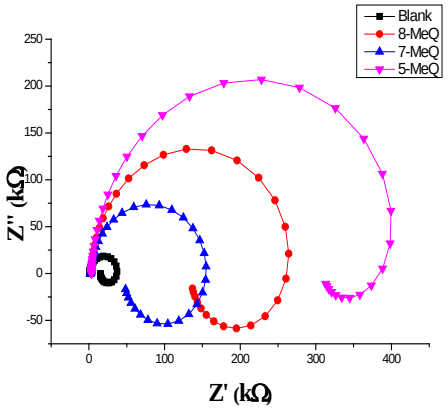

Figure 11: Impedance responses at the metal/acid interface for the corrosion of Al in the absence and in the presence of 0.4g/L 5-MeQ, 7-MeQ and 8-MeQ inhibitors in 0.4M HCl at 303k**.**

The corresponding impedance parameters are presented in Table (6). The increase in R_{ct} values in inhibited systems, which signifies an increase in the diameters of the Nyquist semicircles with a corresponding decrease in the double-layer capacitance (C_{dl}), confirms the corrosion-inhibiting properties of the methyl quinolines. The observed reduction in C_{dl} values, which usually corresponds to alteration of the double layer thickness, can be attributed to the adsorption of the quinolines (with lower dielectric constant compared to the displaced adsorbed water molecules) on the metal/acid interface, thereby protecting the metal from the corrosive effect of the aggressive acids. However, 5-MeQ has the largest amplitude among the three molecules of methyl quinolines tested, as observed in Fig.(11) and the highest percentage inhibition efficiency, as shown in Table (6), which further justified its corrosion inhibition superiority compared to 7-MeQ and 8-MeQ. The amplitude of the Nyqquist plots, and the magnitude and trend of the obtained inhibition efficiencies % IE presented are in agreement with those determined from weight loss measurements.

Table 6: Impedance data for the corrosion of Al in 0.4 M HCl in the absence and presence of 0.4g/L Inhibitor for each system at 303 K.

System	R_{ct} (Ω cm^2)	C_{dl} ($\mu\Omega^{-1}S^n cm^{-2}$)	N	IE%
HCl (Blank)	134.53	3.56	0.86	0.00
5-MeQ	1125.81	1.68	0.98	94.41
7-MeQ	907.42	2.32	0.92	65.87
8-MeQ	1116.52	1.71	0.95	84.25

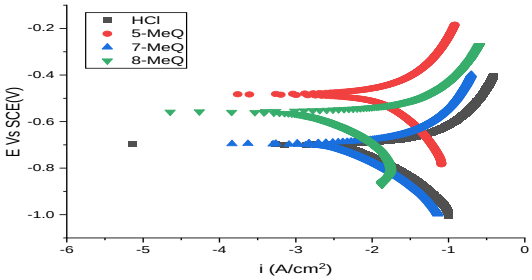

Figure 12: Polarization at the metal/acid interface for the corrosion of Al in the absence and in the presence of 0.4g/L 5-MeQ, 7-MeQ and 8-MeQ inhibitors in 0.4M HCl at 303k**.**

From Table (7), it can be clearly seen that the insertion of Al in the corrodent (HCl) of 0.4M concentration without inhibitor gives a higher value of both the i_{corr} and the corrosion rate at room temperature. Still, they tend to decrease as the inhibitors are introduced in the corrosive solution, which in turn leads to some degree of inhibition. For the first system with 5-MeQ (5-methyl quinoline) of 0.4g/L, a lower i_{corr} value of 17.20µA to 600.00 µA was obtained, while the corrosion rate and inhibition efficiency achieved were 385 mpy and 92.16%, respectively.

The potentiodynamic polarization plots (PDP) (Fig.12) show that the inhibitor affects both the anodic metal dissolution and cathodic hydrogen evolution reactions [39]. For the inhibitors used, the cathodic Tafel lines are parallel for all the inhibitors, which indicates that the inhibitor molecules slightly change the cathodic hydrogen evolution reaction [39].

Table 7: Potentiodynamic polarization data for the corrosion of Al in 0.4 M HCl in the absence and presence of 0.4 g/L Inhibitor for each system at 303 K.

System	BetaA(V/d)	BetaC(V/d)	i_{corr}(µA)	E_{corr}(mV)	CR (mpy)	%IE
Blank	188.2e-3	414.2e-3	617.20	-998.0	11.02e3	0.00
5-MeQ	114.8e-3	116.2e-3	301.90	-799.00	28.20	94.36
7-MeQ	177.4e-3	441.3e-3	424.90	-896.00	8.298e3	69.50
8-MeQ	172.1e-3	330.3e-3	400.00	-835.0	128.4	90.15

The corrosion potential (E_{corr}) values from Table (7) show that the addition of an inhibitor shifts the corrosion potential to the positive side. When the corrosion potential changes noticeably with the introduction of an inhibitor, the inhibitor is claimed to work by blocking the active sites [39]. On the other hand, a negligible change in E_{corr} upon the addition of an inhibitor indicates that the inhibitor works by geometric blocking effect [40]. Hence, in these systems, the inhibitors are believed to work by blocking the active sites. Also, in Table (7), it is observed that the I_{corr} value decreases with inhibitor addition, whereas the E_{corr} increases. Such an increase in Ecorr accompanied by a drop in Icorr is suggestive of corrosion inhibition, and increased surface hydrophobicity, which could be attributed to the inhibitor molecules adsorbed on the Al surface [40-41]. In the present study, the most significant shift caused in the E_{corr} upon inhibitors addition is mostly 45 mV and less, and both cathodic and anodic processes are affected, indicating that the inhibitors indeed work as mixed type[41].

3.6. Scan Electrom Moicrscopy of the Al before and after corrosion:

SEM analysis of the Al before and after corrosion was conducted and presented in Fig. (13 - 17). Fig. (13) shows the morphology of the Al surface prior to the corrosion study, which indicates a smooth and clear surface. Fig. (14) is the micrograph of the same surface after being immersed in 0.4M HCl solution without the inhibitor. Corrosion pits are clearly observed on the surface after 5 hours of immersion, which indicates the effects of the aggressive environment.

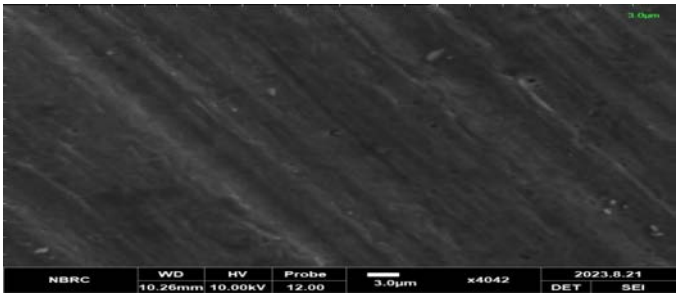

Figure 13: Micrograph of the Raw Al image prior to corrosion study.

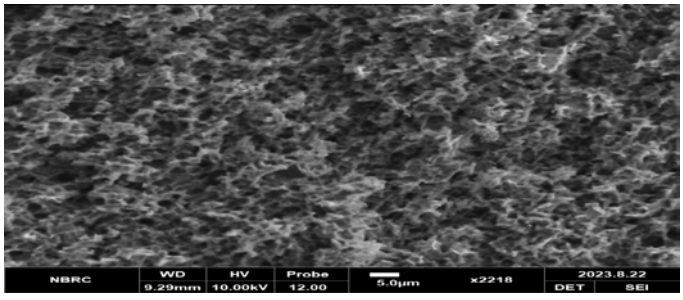

Figure 14: Micrographs of Al after dipping in 0.4M HCl for 5 hour without inhibitor.

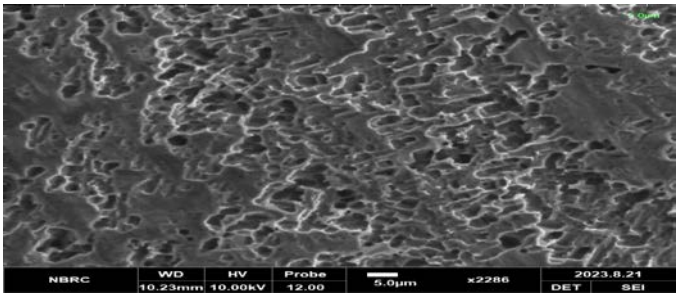

Figure 15: Micrographs of Al after dipping in 0.4M HCl for 5 hour with 0.4g/L 5-MeQ inhibitor.

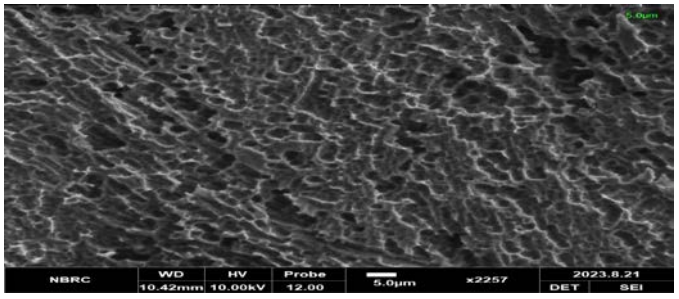

Figure 16: Micrographs of Al after dipping in 0.4M HCl for 5 hour with 0.4g/L 5-MeQ inhibitor.

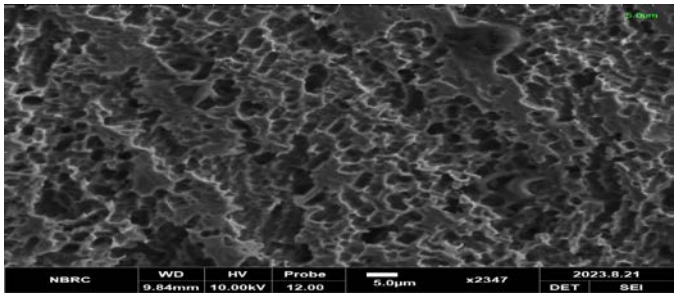

Figure 17: Micrographs of Al after dipping in 0.4M HCl for 5 hours with 0.4g/L 5-MeQ inhibitor.

Fig. (15-17) shows the micrographs of each of the samples immersed in 0.4M with 5-MeQ, 7-MeQ and 8-MeQ inhibitors, respectively. It is clearly seen that the samples immersed in a medium with inhibitors each show a thick layer, which would have been formed from the deposition of corrosion products and inhibitor molecules. The unprotected sample shows the formation of more pits. The surface becomes hydrophobic with the addition of an inhibitor, which also confirms the adsorption of the quinoline derivatives molecules on the surface of the Al and the formation of film to protect the surface, which is typical for mixed inhibitors [42]. However, Fig.(15) shows the surface using a 5-MeQ inhibitor reflects a more uniform layer on the Al-protected surface, which means more corrosion protection than 7-MeQ and 8-MeQ inhibitors. This is consistent with the weight loss and the electrochemical experiments.

3.7. Fourier Transform IR Analysis:

The FTIR spectra of the methyl quinolines derivatives on the surface of Al are shown in Fig.(18-20) for 5-MeQ, 7-MeQ and 8-MeQ, respectively. The appearance of a strong peak around 1353cm^{-1} is due to the methyl group, the peak around 1610cm^{-1} corresponds to the aromatic ring, the nitrogen atom in the molecule has a peak around 1420cm^{-1} and the peak around 1500cm^{-1} stands for the carbon-carbon double bond generally for all the methyl quinoline molecules. The 0.4g/L of the methylquinolines in 0.4MHCl without insertion of the Al coupon clearly shows the presence of methyl group (-CH_3), aromatic ring, nitrogen and carbon-carbon double bond.

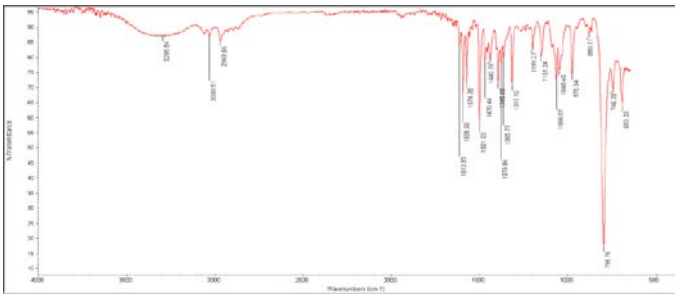

Figure 18: FTIR spectra of Al corrosion products after immersion in 0.4MHCl with and without 0.4g/L 5-MeQ at 303K

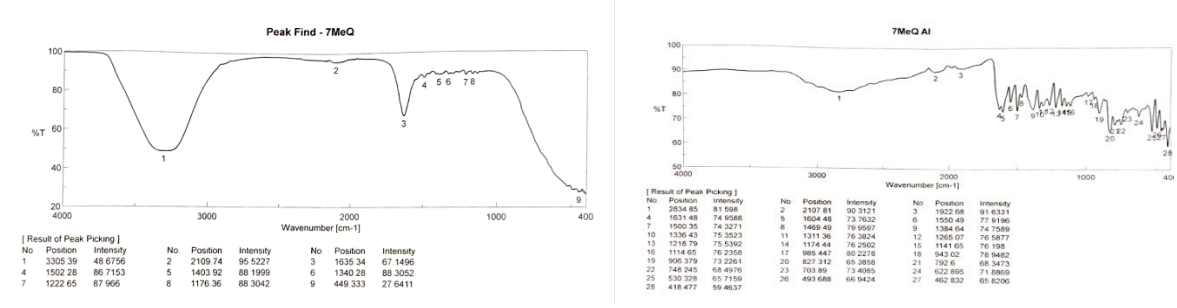

[Result of Peak Picking]

No	Position	Intensity	No	Position	Intensity	No	Position	Intensity
1	3305.39	48.6756	2	2109.74	95.5227	3	1635.34	67.1496
4	1502.28	86.7153	5	1403.92	88.1999	6	1340.28	88.3052
7	1222.65	87.966	8	1176.36	88.3042	9	449.333	27.6411

[Result of Peak Picking]

No	Position	Intensity	No	Position	Intensity	No	Position	Intensity
1	2834.85	81.598	2	2107.81	90.3121	3	1922.68	91.6331
4	1631.48	74.9588	5	1604.48	73.7632	6	1550.49	77.6196
7	1500.35	74.3271	8	1469.49	79.9597	9	1384.64	74.7589
10	1336.43	75.3523	11	1311.36	76.3824	12	1265.07	76.5877
13	1218.79	75.5392	14	1174.44	76.2502	15	1141.65	76.198
16	1114.65	76.2358	17	985.447	80.2278	18	943.02	76.9482
19	906.379	73.2261	20	827.312	65.3858	21	792.6	66.3473
22	748.245	68.4976	23	703.89	73.4085	24	622.695	71.8869
25	530.328	65.7159	26	493.688	66.9424	27	462.832	65.8206
28	418.477	59.4637						

Figure 19: FTIR spectra of Al corrosion products after immersion in 0.4MHCl with and without 0.4g/L 7-MeQ at 303K

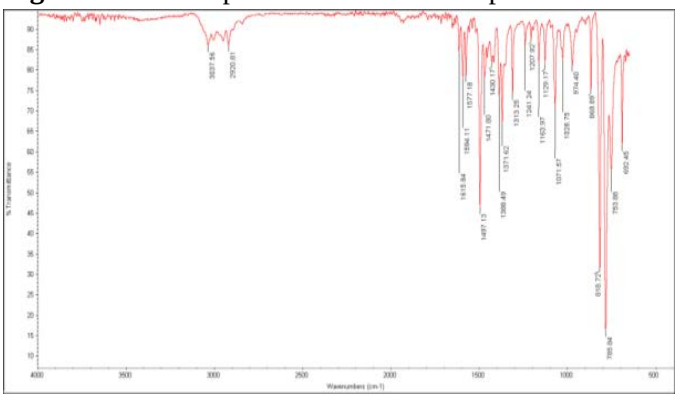

Figure 20: FTIR spectra of Al corrosion products after immersion in 0.4MHCl with and without 0.4g/L 8-MeQ at 303K

However, upon insertion of the Al in the solution, the peak corresponding to -CH_3 stretch at 1353cm^{-1} slightly shifted to 1349cm^{-1} for both 7-MeQ and 8-MeQ, and 1345cm^{-1} for 5-MeQ molecule, the aromatic ring at 1615cm^{-1} changes to 1513cm^{-1}, peak of nitrogen which appears around 1420cm^{-1} shifted to 1415cm^{-1} in 7-MeQ and 8-MeQ, but has disappeared

in 5-MeQ molecule. From the FTIR, Such a shift is attributed to the interaction of the methylquinoline molecules with the metal surface [42]. The high stretching value of the methyl peak and the nitrogen and even the disappearance of the peak of N, which is more with 5-MeQ, is evidence of the bonding of the Al surface with the methyl quinoline molecules. This reaffirmed the fact that the mechanism is both physical and chemical adsorption[43].

3.8. Mechanism of Inhibition

Naturally, the test Al plate before the corrosion study has air passive film of Al oxides on their surface due to oxidation, as shown in equation (17).

$$4Al + nH_2O + 3O_2 \rightarrow 2Al_2O_3(H_2O)n \quad (17)$$

However, the dissolution of the Al in the aggressive medium (acid solution) can be represented in equation (18) [44]

$$Al \rightarrow Al^{3+} + 3e^- \quad (18)$$

The quinoline derivatives used here are the 5-MeQ, 7-MeQ and 8-MeQ, which have the same molecular mass and similar structure. The interaction of Al with these molecules generally involves the formation of a complex between the Al ion, methyl group and nitrogen atoms of the hydroxyquinoline molecule. The complex is hydrophobic and acts as a corrosion inhibitor by blocking the active sites on the Al surface, thus preventing the reaction between the Al and the corrosive medium. The most likely chemical equation for this interaction is presented in the equation (19)

$$Al^{3+} + 3C_9H_9N + 6H_2O \rightarrow [Al(C_9H_9N)_3(H_2O)]^{3+} + 3OH^- \quad (19)$$

Here, the Al ion (Al^{3+}) is complexed with three molecules of methyl quinoline and three molecules of water, forming a positively charged complex that is highly hydrophobic. Furthermore, from the quantum chemical parameters and the FTIR peak, the difference in the inhibition efficiency shown by the molecules, despite having the same mass and structure, is believed to come from the orientation of the substituent ($-CH_3$) position on the parent quinoline molecule. Intra-molecular hydrogen bond is suspected to occur in 7-MeQ and 8-MeQ, which leads to poor donation of the vacant site from the methyl group in the formation of the metal complex. This lowered the inhibition performance. The stronger the intra-molecular hydrogen bond, the slower the complex formation, hence poor inhibition efficiency [45]. At position 5, the methyl group does not likely form an intra-molecular hydrogen bond. As a result, 5-MeQ readily formed a complex with the Al and displayed excellent corrosion inhibition performance compared to the other two molecules.

Conclusion

The influence of methyl substituent position on quinoline used as a corrosion inhibitor for Al in hydrochloric acid was successfully investigated experimentally and theoretically. Out of the three methyl quinoline derivatives(5-methyl quinoline, 7-methyl quinoline and 8-methyl quinoline), 5-methyl quinoline showed the highest corrosion inhibition efficiency under all conditions. The results obtained from mass loss, potentiodynamic polarisation and impedance measurement support these observations. The theoretical study has justified the results of all investigations. The position of the methyl substituent on the quinoline molecule showed some influence on the corrosion inhibition performance of the Al in an acidic medium. Scanning electron micrographs confirmed that 5-MeQ has more uniform blockage of the etching sites on the acid-stricken Al slabs. Based on this, we can say that 5-MeQ is an effective corrosion inhibitor because it forms a stronger bond with the metal surface and lowers the activation energy for the corrosion reaction. This suggests that 5-MeQ is a promising candidate for use in industrial applications where corrosion prevention is needed. From the FTIR, the significant shift in wavenumber is attributed to the interaction of the methylquinoline molecules with the metal surface. The high stretching value of the methyl peak and the nitrogen and even the disappearance of the peak of N, which is seen with 5-MeQ, is evidence of the bonding of the Al surface with the methyl quinoline molecules. This reaffirmed that the mechanism is a mixed adsorption.

Acknowledgment: Authors are thankful to the Department of Chemistry, Federal College of Education (Technical) Bichi, P.M.B. 01000 Kano, Nigeria, for providing research facilities for the above project.

Reference:

1. A. G.Sayed, A. M. Ashmawy, W. E. Elgammal, S. M. Hassan, & M. A. Deyab, *Sci. Rep., 13(1),* 13761. **(2023)**
2. E. A. Arazua and B. B. Adeleke. *J. Appl. Sci. Environ. Manage. Vol. 23(10)* 1819-1824 **(2019).**
3. J. H. Bao, H. Zhang, X. Zhao, and J. Deng, *Chemical Engineering Journal*, *341,* 146 – 156, **(2018).**
4. A. U. Bello, A. Uzairu and G. A. Shallangwa, *Port. Electrochim. Acta*. *38(6)*, 377-386, **(2020).**
5. B. E. Brycki, I. H. Kowalczyk, A. Szulc, O. Kaczerewska, & M. Pakiet, *Appl. Charact. Surfactants*, 97-155. **(2017).**
6. C. J. Casewit, K. S. Colwell, and A. K. Rappé, *J. Am. Chem. Soc., 114:*10046–10053 **(1992b).**
7. H. J. Chen, T. Hong, and P. Jepson, *Corrosion 2000*, 00035. **(2022).**
8. M. Chi., and Zhao, Y.P. (2019). M. Chi, and, Y.P. Zhao, *Comput. Mat. Sci., 46*(4), 1085-1090 **(2009)**
9. V. Cicek. and B. Al-Numan(2021), *Fundamentals, Methodologies, and Industrial Applications*, 1-19
10. S. Deng, X. Li, & H. Fu, *Corros. Sci., 53(2),* 760-768, **(2011).**
11. N. O. Eddy, S. A. Odoemelam, and A. O. Odiongenyi, *Green Chem. Lett. Rev.,2(2):* 111-119, **(2009)**
12. E. E. Oguzie, Y. Li, & F. H. Wang, *Electrochim. Acta*, *53*(2), 909-914. **(2007).**
13. A. EI-Awady, B. A. Abd-EI-Nabey, and S. G. Aziz, *J. Electrochem. Soc., 139(8)*: 2149-2154. **(1992).**
14. E. E. Oguzie, Y. Li, & F. H. Wang, *Electrochim. Acta*, *53*(2), 909-914. **(2007). (Repreated numbers)**

15. U. F. Ekanem, S. A. Umoren, I. I. Udousoro and A. P. Udoh, *J. Mater. Sci., 45(20)*: 5558-5566. **(2010).**
16. M. Elfaydy, H. Lgaz, R. Salghi, M. Larouj, S. Jodeh, M. Rbaa, H. Oudda, K. Toumiat and B. Lakhrissi, *J. Mater. Environ. Sci., 7(9),* 3193-3210, **(2016).**
17. M. M. El-Rabiee, N. H. Helal, G. M. Abd El-Hafez, and G. A. Badawy, *J. Alloys Compd,459*, 466–471, **(2008).**
18. C. K. Enenebeaku, Ph.D Thesis. Federal University of Technology, Owerri, **(2011).**
19. E. A. Erazua and B. B. Adeleke, *J. Appl. Sci. Environ. Manage., Vol. 23(10),* 1819-1824, **(2019).**
20. A. U. Ezeoke, O. G. Adeyemi and O. A. Akerele, *Int. J. Electrochem. Sci., 7*, 534, **(2012).**
21. J. Feng, R. B. Pandey, R. J. Berry, B. L. Farmer, R. R. Naik, and H. Heinz, *Soft Matter. 7,* 2113-2120, **(2010).**
22. L. Feng, H. Yang, and F. Wang, *Electochimica Acta, 58*, 427-436, **(2011).**
23. C. Fiaud, Theory and Practice of Vapour Phase Inhibitors, in A Working Party Report on Corrosion Inhibitors, London, U.K., The Institute of Materials, pp.1– 11. **(1994).**
24. M. G. Fontana,. Corrosion Engineering, New York, McGraw-Hill Book Company Biochromy, natural colouration of living things. University of California Press, **(1986)**
25. L. Fragoza-Mar, O. Olivares-Xometl, M. A. Domínguez-Aguilar, E. A. Flores, P. Arellanes- Lozada, and F. Jiménez-Cruz, *Corros. Sci., 61*, 171–184, **(2012).**
26. R. Fuchs-Godec, and G. Zerjav, *Acta Chim. Slov., 56*, 78-85, **(2009).**
27. R. Gasparac, C. R. Martin, and E. Stupnisek-Lisac, *J. Electrochem. Soc., 147(2)*, 548-551, **(2000a).**
28. R. Gasparac, C. R. Martin, E. Stupnisek-Lisac, and Z. Mandic, *J. Electrochem. Soc., 147(3)*, 991-998, **(2000b).**
29. M. Goyal, S. Kumar, I. Bahadur, C. Verma, and E. E. Ebenso, *J. Mol. Liq., 256*, 565–573, **(2018).**
30. L. Hamadi, S. Mansouri, K. Oulmi, and A. Kereche, Egyptian Journal of Petroleum, vol. 27, no. 4, pp. 1157–1165, **(2018).**
31. S. Kadapparambil, K. Yadav, M. Ramachandran, & N. Victoria Selvam, *Corros. Rev., 35(2),* 111-121, **(2017).**
32. K. F. Khaled and N. S. Abdel-Shafi, *Int. J. Electrochem. Sci., 6,* 4077 – 4094, **(2011).**
33. M. Larif, S. Chtita and A. Adad, *Int. J., 3(12),* 32-42, **(2013).**
34. L. C. Murulana, A. K. Singh and S. K. Shukla, *Ind. Eng. Chem. Res., 51(40),* 13282-13299, **(2012).**
35. Y. Qiang, S. Zhang, B. Tan, and S. Chen, *Corros. Sci.,133*, 6–18, **(2018).**
36. S. Rajendran, J. Jeyasundari, P. Usha, J. A. Selvi, B. Narayanasamy, A. P. P. Regis, and P. Rengan, *Port. Electrochim. Acta, 27(2),* 153–164, **(2009).**
37. A. K. Satapathy, G. Gunasekaran, S. C. Sahoo, K. Amit, and P. V. Rodriquez, *Corros. Sci.,51(12),* 2848–2856, **(2009).**
38. N. Soltani, Tavakkoli, M. Khayatkashani, and M. R. Jalali, *Corros. Sci.,62*, 122–135, **(2012).**
39. D. E. J. Talbot and J. D. R. Talbot, *Corrosion Science and Technology*, 3rd ed. New York: Taylor and Francis, 159–194, **(2018).**
40. K. Tebbji, N. Faska, A. Tounsi, and H. Oudda, *Mater. Chem. Phys.,106(2–3)*, 260–267, **(2007).**
41. C. Verma, L. O. Olasunkanmi and E. E. Ebenso, *J. Phys. Chem., 120(21)*, 11598, **(2016).**
42. C. Verma, M. A. Quraishi, and E. E. Ebenso, *Surf. Interfaces, 21*, 100634, **(2020).**
43. V. C. Sandu, I. Dumbrava, A. M. Cormos, A. Imre-Lucaci, C. C. Cormos, P. D. Cobden, & R. de Boer, *Comput.-Aided Chem. Eng. 46*, 751-756, **(2019).**
44. H. Zhang, Y. Chen, Z. Zhang, Zhang, *Results Phys., 11*, 554-563. **(2018).**
45. C. Zhu, H. X. Yang, Y. Z. Wang, D. Q. Zhang, Y. Chen, and L. X. Gao, *Ionics, 25(3),* 1395–1406, **(2018).**

Received:Febraury 19th 2024 **Accepted: March 11th 2024**